JOURNAL OF Applied Polymer SCIENCE

Influences of different preparation variables on polymeric membrane formation via nonsolvent induced phase separation

Catharina Kahrs,[1,2] **Thorben Gühlstorf**,[1,3] **Jan Schwellenbach**[1]

[1]Sartorius Stedim Biotech GmbH, 37079, Goettingen, Germany

[2]Institute for Technical Chemistry, Leibniz University Hannover, 30167, Hannover, Germany

[3]Faculty of Computer Science and Engineering, Frankfurt University of Applied Sciences, 60318, Frankfurt/Main, Germany

Correspondence to: C. Kahrs (E-mail: catharina.kahrs@sartorius.com)

ABSTRACT: This work presents a comparative study on the formation of polyethersulfone ultrafiltration membranes via nonsolvent-induced phase separation (NIPS) in two different solvent systems. *N*-methyl-2-pyrrolidone was chosen as conventional solvent and 2-pyrrolidone as a greener alternative. The overall objective was to obtain a mechanistic clarification of the membrane formation process in dependence of the most important controlling parameters. By performing different series of experiments, it was possible to determine the differences between the two solvents regarding the effects of variations in nonsolvent additives, polymer concentration, and precipitation conditions. It was found that a raising concentration of several nonsolvents, the increase of the polymer concentration and changes in the precipitation conditions can suppress the formation of macrovoids, regardless of the applied solvent. In contrast, differences were observed with regard to the performance of the membrane prototypes. This study improves the understanding of membrane formation via NIPS and identifies the effects of different variables. It shows that the choice of the solvent is essential for the dominating formation mechanisms and therefore for the resulting membrane features. It also proves that green solvents can substitute hazardous solvents if the influencing variables are well-understood in order to control them for obtaining desired membrane properties. © 2019 The Authors. *Journal of Applied Polymer Science* published by Wiley Periodicals, Inc. J. Appl. Polym. Sci. **2020**, *137*, 48852.

KEYWORDS: membranes; microscopy; separation techniques

Received 12 September 2019; accepted 9 December 2019

DOI: 10.1002/app.48852

INTRODUCTION

Nowadays, filtration with polymeric membranes is an important operation unit for various separation processes in different application fields.[1–5] Depending on the purpose of the filtration process as well as on the correspondingly valid regulatories, the membranes have to fulfill a large variety of different demands.[6–8] However, in order to enable the control of the resulting membrane features for the obtainment of desired product properties, it is necessary to well understand the mechanisms of membrane formation and their influencing variables.[9–11]

One of the most frequently used materials for the production of polymeric membranes is polyethersulfone (PES).[12,13] In contrast to other commonly applied polymers such as polysulfone (PSf), cellulose acetate (CA), polyvinylidene fluoride (PVDF), or polyamide (PA), it stands out due to particular characteristics. The favoring properties of PES include a high glass transition temperature of 225 °C, a large chemical, mechanical, and thermal resistance, an excellent biocompatibility, as well as the potential application within a large pH range.[14–17] Furthermore, the use of PES enables an easy fabrication of membranes with a large range of different pore sizes, which can be applied in several different modules and configurations.[10] This is the reason why PES membranes are used in several different fields such as gas separation, water processing, medical treatments, and biotechnology.[17–19] Specific applications include the sterilization of drinking water, the concentration of juices, hemodialysis, drug delivery, as well as the purification and concentration of biopharmaceutical drugs with a biological source.[20–22] In dependence of the

Additional Supporting Information may be found in the online version of this article.

[Corrections added on 23 March 2020, after first online publication: Figure 4 and Conclusion section have been updated.]

respective application, a PES membrane has to possess certain features with respect to pore size, structure, and performance. In order to gain the desired membrane characteristics the production process of PES membranes has to be strictly controlled. The main controlling factors include the composition of the membrane dope solution on one hand, and the process parameters on the other hand.[19]

Nonsolvent induced phase separation (NIPS) is one of the most frequently applied approaches for PES membrane fabrication.[23–25] It enables the production of asymmetric structures with a large range of different characteristics, since the resulting membrane properties can be largely controlled if the formation process is well understood.[26–29] During NIPS a homogenous PES solution is immersed into a nonsolvent bath.[11] The diffusive exchange between the solvent from the polymer film and the nonsolvent from the precipitation bath changes the composition within the polymer film, till phase separation occurs.[16,30,31] Until solidification sets in different structure forming mechanisms occur, which result in different morphologies.[16,32,33] Apart from the composition path through the phase diagram, the occurring mechanism is ultimately dependent on the entry point into the miscibility gap.[34,35] When the system directly enters the metastable region binodal decomposition occurs, which induces the formation of a closed-cellular, an open-cellular or a nodular morphology. In contrast, spinodal decomposition occurs if the entry into the miscibility gap occurs directly through the critical point into the unstable region, leading to a bicontinuous structure.[34,36,37] If the structure is fixed immediately after the phase separation has occurred, one of the characteristic membrane morphologies can be observed (Figure 1).

In this special case, the actual membrane morphology is ultimately determined by the point of entry into the miscibility gap.[36] However, in most cases, different coarsening mechanisms take place after the solution has reached the two-phase region, so that an unambiguous conclusion from the final structure to the original decomposition mechanism is almost impossible.[24,38] Especially the formation of larger voids is caused by different coarsening effects.[39–42] In this context, the speed and duration of the diffusional solvent replacement from the polymer film determines if the membrane morphology is either sponge-like, finger-like, or a distinct mixture of both.[43–45] Consequently, the nascent structure formed after the onset of phase separation should not be regarded as static, since structure-forming effects can result from a steady mass transfer until solidification is reached.[46] If a critical viscosity is reached, the polymer solution turns into a gel state and solidifies, as coalescence and other coarsening mechanisms are no longer possible.[47–50]

Apart from the thermodynamics of the system, the phase separation process is dependent on the kinetics.[51–53] Especially the diffusion rate, which determines the exchange speed between solvent and nonsolvent, plays a critical role for the change of the solution composition and for the promotion of certain mechanisms such as coalescence, consequently resulting in different morphologies.[14,54–56] This is why the formation of the final membrane structure can be manipulated by alterations in the temperature, which affects both, kinetics and thermodynamics of the system.[57–60] Furthermore, it can be influenced by variances in the viscosity through compositional changes, as the viscosity has a high impact on the diffusion rate.[61,62] Another important influencing factor is the choice of the solvent. Depending on the affinity between the solvent and the chosen nonsolvent, the diffusional exchange can be regulated.[14,63,64] Additionally, the solubility of the polymer in the solvent is a relevant factor. On one hand, it has been shown that the choice of the solvent strongly impacts the viscoelastic properties of the polymer solution, which consequently alters the diffusional processes during membrane formation.[29,65] On the other hand, the miscibility gap is strongly dependent on the solvent.[17,29,65] Therefore, the thermodynamic basis for the phase separation can be tuned by applying different solvents.

Currently, an emerging topic is the substitution of potentially hazardous solvents such as *N*-methyl-2-pyrrolidone (NMP) through greener alternatives.[66–70] The aim of this substitution is the minimization of the environmental impact and the simultaneous maximization of the membrane fabrication sustainability, in order to meet the criteria of green chemistry.[71–74] However, for the replacement of potentially harmful solvents, a profound understanding of the solvent impact is crucial. This is why a comparative investigation of several controlling variables was conducted by performing all experiments in a hazardous solvent and a potential greener alternative.

The listed mechanisms contributing to the structure formation of the membrane are part of controversial discussions.[8,24,53,75] Individual physicochemical phenomena can be described in isolation, however, quantitatively and qualitatively predictions of the final membrane structure are hardly possible due to the large

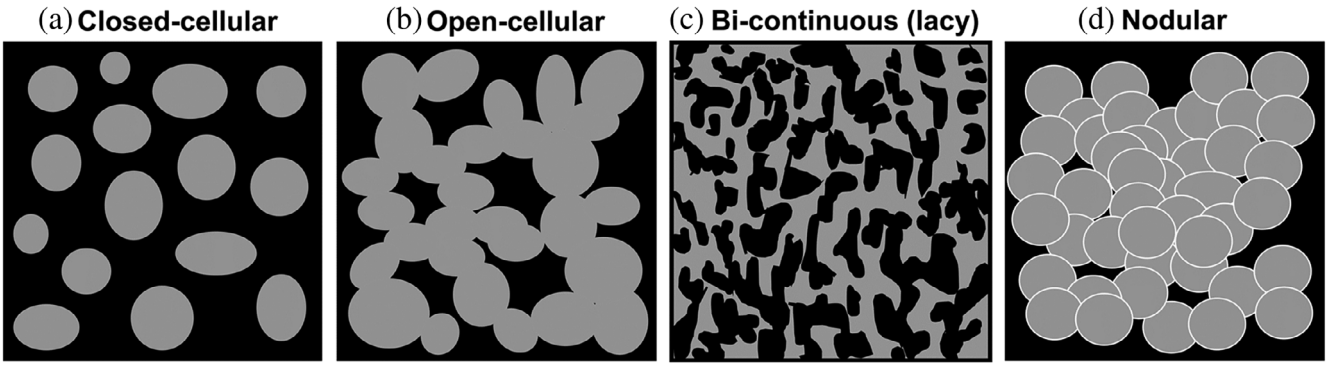

Figure 1. Schematic depiction of the four most common membrane morphologies developing during the phase separation of polymeric solutions.

number of factors and dependencies of the formation mechanisms.[8,24,42,53,75,76] Although qualitative correlations have been published in the literature, they are yet predominantly discussed on the basis of investigations limited to individual casting solution systems. This is why an empirical approach was chosen to qualitatively identify the influencing factors and their effects on membrane morphology and performance in order to obtain the currently missing holistic picture on membrane formation via NIPS. Through targeted variations of the casting solution composition and the manufacturing conditions, a broad database should be created by applying selected characterization methods to identify the physicochemical relationships of membrane formation. In this case, the polymer concentration, the concentration of three different nonsolvents, the precipitation bath composition and the precipitation temperature were varied to affect the thermodynamic and kinetic properties of the membrane formation process. Furthermore, NMP was applied as a good but hazardous solvent, whereas 2-pyrrolidone (2P) was used as a greener alternative with a poorer dissolving power for PES. All variations were conducted comparatively in both solvent systems. By doing so, a comprehensive picture should be established in order to broaden the understanding of the interplay between different factors, which affect the kinetics and the thermodynamics of the phase separation process. Consequently, this study shall enable an improved morphological control of the membrane structure. Furthermore, since the membrane performance is strongly related to the membrane morphology, this enhanced understanding of the membrane formation process shall facilitate to fulfill the requirements of regulatories and users of membranes.

EXPERIMENTAL

Materials

The membrane-forming polymer PES was obtained from BASF (Ludwigshafen, Germany). In order to dissolve the polymer, NMP and 2P were purchased from Carl Roth (Karlsruhe, Germany). Polyvinylpyrrolidone (PVP) with a molecular weight of 1400 kDa was purchased from BASF (Ludwigshafen, Germany) and added to the casting solutions as a hydrophilic additive. Furthermore, reverse-osmosis (RO) water from Sartorius Stedim Biotech (Goettingen, Germany) was applied as a nonsolvent additive within the casting solution, as well as the phase separation inducing agent in the precipitation bath. Further applied nonsolvent additives were glycerol and acetic acid, both acquired from CG Chemicals (Laatzen, Germany). For membrane permeability and retention measurements, a 20 mM potassium phosphate buffer (pH 7.0) was used. This buffer was prepared from stock solutions of di-potassium hydrogen phosphate and potassium dihydrogen phosphate, both acquired from Carl Roth (Karlsruhe, Germany). The alternative precipitating agent isopropanol was acquired from CG Chemicals (Laatzen, Germany).

Preparation of Membrane Dope Solutions

Membrane dope solutions with varying solution compositions were prepared. Every single composition was fabricated twice, where the replicating formulations only differed in the type of the applied solvent. In addition to the impact of PES concentration variations from 15 to 20 wt%, the influence of different amounts of water, glycerol, and acetic acid as nonsolvent additives was investigated. In both solvents, the amount of glycerol was varied from 0 to 5 wt%, whereas the share of acetic acid ranged from 0 to 7.5 wt%. In contrast, the corresponding amounts of water within the casting solution were adapted to the solvent-dependent location of the miscibility gap. In case of NMP, the water concentration was varied between 7 and 9.25 wt %, whereas in case of 2P, the concentration ranged between 3.5 and 5.75 wt% water. The applied membrane preparation conditions are summarized in Table I. For a list with the exact compositions of each polymer solution refer to the supporting information (refer to Table S1 to Table S4).

Table I. Casting Solution Compositions for the Preparation of PES Membrane Prototypes With Variations in the Concentration of Acetic Acid Using NMP and 2P as Solvents for the Preparation of the Dope Solutions

Samples (N: NMP / P: 2P)	Variable		Fixed parameter [wt%]	Precipitation bath	Precipitation temperature
N1–N5 P1–P5	Water [wt%]	7.5, 8.0, 8.5, 9.0, 9.25 (N) 3.5, 4.0, 4.5, 5.0, 5.75 (P)	PES: 16.88 PVP: 0.84	Water	20 °C
N6–N8 P6–P8	PES [wt%]	15, 18, 20	PVP: 0.84 Water: 9.0 (N) Water: 5.0 (P)	Water	20 °C
N9–N11 P9–P11	Glycerol [wt%]	0.0, 2.5, 5.0, 7.5	PVP: 0.84 Water: 7.5 (N) Water: 3.5 (P)	Water	20 °C
N12–N15 P12–P15	Acetic acid [wt%]	0.0, 2.5, 5.0, 7.5	PVP: 0.84 Water: 7.5 (N) Water: 3.5 (P)	Water	20 °C
N1 P1	Precipitation conditions	water 20 °C, water 40 °C, IPA-water 20 °C	PES: 16.88 PVP: 0.84 Water: 7.5 (N) Water: 3.5 (P)	Water or IPA-water	20 °C or 40 °C

For dope solution preparation, the water content of each raw material was determined. In case of the solid components PES and PVP, the determination was carried out with a moisture analyzer, while the water content of the liquids was analyzed via Karl-Fisher titration (KF Ti-Touch, Metrohm GmbH & Co. KG, Filderstadt, Germany). Under consideration of the water amount, which is introduced trough the raw materials, the remaining volume of needed RO-water as well as the proportion of the respective solvent was poured into a 500 mL twin-neck flask (Carl Roth, Karlsruhe, Germany) and then preheated to 60 °C in a tempered oil bath. Subsequently, the solid components were added under constant stirring at 250 rpm using a RW20 overhead stirrer (IKA, Staufen, Germany). In all cases, PVP was added first and PES was added last. The dope solutions were stirred overnight to guarantee a homogenous mixing. Finally the polymer solutions were degassed in an oven for 2 h at 50 °C. For membrane preparation, the polymer solutions were cooled down to room temperature.

Cloud Point Experiments

Cloud point experiments were performed for both solvent systems with water as nonsolvent. The prepared polymer solutions were filled into a reactor (HWS, Mainz, Germany) and tempered to 20 °C. By application of an automatic titration system (Metrohm 900 Touch Control, Metrohm 846 Dosing Interface, Metrohm 807 Dosing Unit and Metrohm 800 Dosino, Metrohm GmbH and Co. KG, Filderstadt, Germany), 0.03 mL/min of water was added to the tempered solution under constant stirring at 300 rpm (IKA overhead stirrer RW20, IKA, Staufen, Germany). During this procedure, the transmitted light was measured as a function of time by a photometric sensor (Metrohm 662 Photometer, Metrohm GmbH and Co. KG, Filderstadt, Germany). The measurement was stopped when the light transmitted dropped below a value of 5%. Afterward the composition at the inflection point of the titration data was determined using Origin 2018b (Northampton, MA), since this point represents the cloud point of the solution. For each system solutions with different polymer concentrations were analyzed and used to extrapolate a binodal curve as described by Smolder *et al.*[77]:

$$\ln\frac{\phi_{NS}}{\phi_P} = b\cdot\ln\frac{\phi_S}{\phi_P} + a \tag{1}$$

where ϕ_{NS} is the weight fraction of the nonsolvent, ϕ_P is the weight fraction of the polymer, ϕ_S is the weight fraction of the solvent, and a and b are the constants resulting from the equation of the linear regression from the experimentally determined cloud point data.

Dynamic Casting Solution Viscosity

By using a HAAKE falling ball viscometer (ThermoFisher Scientific, Waltham, MA), the dynamic viscosity of each dope solution was measured at 25 °C. The casting solution and an appropriate nickel-steel ball, with respect to the expected viscosity range, were filled into the inner pipe of the double-walled viscometer. The solution was tempered to 25 °C for at least 15 min by pumping preheated water through the outer casing of the viscometer using a thermostat (Lauda, Lauda-Koenigshofen, Germany). The actual measurement was conducted by stopping the falling time of the ball for a certain distance in a fivefold replication. Finally, the dynamic viscosity was calculated:

$$\eta = \frac{t_m\cdot(\varphi_B-\varphi_S)\cdot K}{1000} \tag{2}$$

where η is the dynamic viscosity (Pa·s), t_m is the average falling time of the ball (sec), φ_B is the density of the ball (g/cm^3), φ_S is the density of the dope solution (g/cm^3), and K is the ball constant (mPa·cm^3·g^{-1}), which was determined during the calibration of the ball.

Preparation of Membrane Prototypes

The prepared dope solutions were used to fabricate different membrane prototypes. Using a casting rake with a defined thickness of 250 µm, the polymer solutions were equally coated onto a glass support at room temperature. After coating, the casting film was immediately precipitated by immersing the support plate with the polymer film into a precipitation bath consisting of nonsolvent either tempered to 20 or 40 °C. The nonsolvent in the precipitation bath was either RO-water or isopropanol. The samples remained in the nonsolvent bath for five minutes to ensure a complete exchange of solvent and nonsolvent, resulting in a self-initiated detaching of the membrane from the glass support. Following this, the prototypes were soaked with RO-water containing 40 wt% glycerol in order to prevent a collapse of the pore network during storage. Subsequently, the membranes were placed into an oven for 10 min at 50 °C and finally stored in airtight sealed bags until further used.

Scanning Electron Microscopy

In preparation for scanning electron microscopy, a piece of the respective membrane prototype was cut and rinsed with RO-water for 15 min to extract the remaining glycerol from the membrane structure. In order to prepare membrane cross-sections, the wetted samples were immersed into liquid nitrogen and smoothly broken using a razor blade. The prepared cross-sections were placed into a sample holder, fixed with conductive silver and sputter coated with argon. Finally, the cross-section images were recorded at high vacuum and a voltage of 12.5 kV by using a FEI Quanta 200 ESEM (ThermoFisher Scientific).

Mechanical Stability

The bursting pressure is defined as the pressure, which is needed to rupture the membrane. It provides information about the mechanical stability of a sample. Since the bursting pressure strongly depends on the membrane thickness, it was normalized to the thickness of the respective sample. This is why the thickness of each sample was measured previous to the actual bursting pressure determination. Since both measurements were run in triplicates, three membrane samples with a diameter of 47 mm were cut from different locations distributed across the whole membrane sheet. Afterward, the thickness of the dry membrane blanks was measured by means of a thickness gauge (Hahn + Kolbe Group, Ludwigsburg, Germany). Following that, the same membrane samples were wetted with water and placed with the skin-side down into the bursting pressure device. The measurement was started by moving the plunger with the pressure supply directly onto the membrane blank. Subsequently, the pressure was continuously increased until the membrane cracked with an

audible bang. The pressure gauge remained at the highest achieved pressure so that the bursting pressure could be read from the meter of the device.

Membrane Permeability

The membrane samples were tested in terms of their permeability. Therefore, a 20 mM phosphate buffer (pH 7.0) was prepared in RO-water. A sample of the respective membrane was cut out of the prepared membrane sheet with a diameter of 26 mm. Together with a fibrous support, it was then integrated into a 10 mL of stirring cell (Sartorius Stedim Biotech GmbH, Goettingen, Germany). The cell was filled with the prepared buffer and was closed with a lid having a connection to the pressure supply. Subsequently, the filtration was started by applying a pressure of 1 bar to the stirring cell. After collecting 10 mL of the filtrate, which was filtered over the effective filter area of 3.8 cm^2 at a stirring speed of 1100 rpm (IKA color quid, IKA, Staufen, Germany), the pressure supply was switched off and the filtration time was recorded. Finally, the filtration time and the operation conditions were used to calculate the permeability:

$$J = \frac{V_F}{A_M \cdot t \cdot p} \tag{3}$$

where J is the membrane permeability ($L \cdot m^{-2} \cdot h^{-1} \cdot bar^{-1}$), V_F is the filtration volume (L), A_M is the effective filtration area of the membrane (m^2), t is the filtration time (h), and p is the applied pressure (bar).

Protein Retention Capacity

Lysozyme (Lot. 235 225 855, Carl Roth, Karlsruhe, Germany) was applied as model protein for determining the protein retention capacity of the prepared membrane prototypes. Using the 20 mM potassium phosphate buffer (pH 7.0) as diluent, a 0.2 g/L protein suspension was prepared and homogenized on a magnetic stirrer (IKA color squid, IKA, Staufen, Germany) at 250 rpm, until the protein was completely dissolved. The stirring cells from the permeability determination were used again to test the protein retention on the same membrane samples. The remaining solution from the previous measurement was completely removed from the cell, and it was then filled again with 10 mL of the protein solution. The cells were closed and a pressure of 1 bar was applied to start the filtration, which was carried out on a magnetic stirrer (IKA color squid, IKA, Staufen, Germany) at a stirring rate of 1100 rpm in order to simulate cross flow conditions. After collecting 5 mL of the filtrate in a designated test tube, the filtration was stopped and the filtration time was recorded. Before the cell was filled again with 5 mL off the pure buffer, it was rinsed twice with buffer to remove protein residues from the measuring module. In order to collect the protein solution remaining downstream of the membrane sample within the tubing of the measuring module, the filtration was continued at 1 bar and 1100 rpm until a final filtrate volume of 7.5 mL was reached. Ultimately, the protein concentrations in the initial solution and the collected filtrates were determined by UV spectrometry (Infinite® 200 PRO, Tecan, Maennedorf, Switzerland) at a wavelength of 280 nm. Based on the proportionality between the UV absorption of the protein and its concentration, the lysozyme retention was calculated by comparing the concentration in the initial solution to those of the respective filtrate:

$$R = 1 - \frac{c_p}{c_f} \cdot 100 \tag{4}$$

where R is the protein retention (%), c_p is the protein concentration in the filtrate (g/L), and c_f is the protein concentration in the initial solution (g/L).

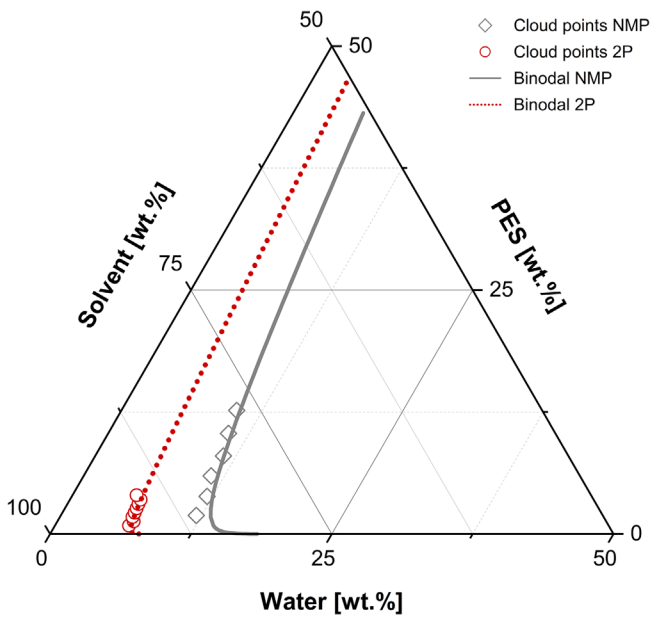

Figure 2. Experimental cloud point data and the thereof extrapolated binodal curves for PES/NMP/water and PES/2P/water at 20 °C. [Color figure can be viewed at wileyonlinelibrary.com]

RESULTS AND DISCUSSION

Location of the Miscibility Gap

Cloud point titrations have frequently been used to determine the miscibility gap of ternary polymeric systems.[16,30,78] It has previously been shown that the location of a system's heterogeneous region is dependent on the combination of polymer, solvent, and nonsolvent.[23,79] In order to gain information on the thermodynamic fundamentals of the PES/NMP/water and PES/2P/water systems applied in this study, cloud point experiments were performed for both systems and used to extrapolate the border between homogeneous and heterogeneous region. The experimental determined cloud points as well as the extrapolated binodal curve for each of the two systems are shown in the phase diagram depicted in Figure 2.

The system consisting of PES/NMP/water has been frequently studied in the past,[17,48,80,81] whereas the phase diagram for PES/2P/water has not been reported before. The experimentally determined phase boundaries for the NMP system in this study agree with the results, which have been previously reported in the referred literature. In comparison to the NMP system, the system with 2P has a larger miscibility gap. This indicates that the thermodynamic stability of 2P solutions is lower than the one of NMP solutions. Therefore, less water is needed to induce the liquid–liquid demixing in the 2P system, so that in contrast to

PES solutions prepared with NMP the phase inversion occurs earlier. It was found that the amount of water, which can be added before phase separation occurs significantly differs between the two studied solvent systems. Based on the extrapolated cloud point data, the water amount, which is needed to induce phase separation in the NMP system lies between 10 and 20 wt%, where the exact amount depends on the polymer concentration. In contrast, for 2P the range lies between 3 and 8 wt%. As a consequence of the different thermodynamic stabilities, it can be expected that the resulting membrane structures differ in dependence of the solvent which is used.

Control of the Morphological Structure by Nonsolvent Additives

It is reported in the literature that the addition of nonsolvent additives to the polymeric dope solution can suppress the formation of finger-like structures.[10,35] However, the knowledge of the impact of nonsolvent additives is limited. This is why in this study the influences of three selected nonsolvents with varying concentrations were investigated comparatively in two different solvent systems. More precisely, changing ratios of water, glycerol, and acetic acid were added to the membrane dope solutions prepared with NMP or 2P, respectively, and consequently their effects were examined with regard to the morphology of the resulting membrane prototypes. In order to study the morphology of the membranes, scanning electron microscopy was applied. Aiming to gain insights into the morphology of both, retentive layer and support layer, cross-section images of each membrane type were recorded.

Figure 3 shows the cross-sections of membranes, which were prepared with NMP as solvent and with different water concentrations in the dope solutions varying from 7.5 to 9.25 wt%. It could be observed that the increase of the water content within the polymer solution lead to a suppression of the finger-like structure, and thus conversely promoted the formation of a sponge-like structure. The more water was added, the more the number of finger-like cavities and macrovoids decreased. Furthermore, the appearance of the cavities within the membrane cross-section moved toward the bottom of the membrane when the water concentration was raised. At the same time, the size of the macrovoids was visibly reduced. This can be explained by the impacts of the water content on the thermodynamic and kinetic aspects of phase separation. In general, the addition of water to the polymer solution moves the starting point of the solution closer to the miscibility gap. If the position of the starting composition is already located close to the miscibility gap, only small amounts of the entering nonsolvent are required to initiate the phase separation across the entire casting solution profile. Therefore, the proportion of the polymer film, which remains stable, since its composition stays within the homogenous region after immersion into the precipitation bath, decreases when the distance to the miscibility gap is reduced. Furthermore, an increase of the nonsolvent concentration within the casting solution will not only reduce the proportion of the film, which remains stable, but also the residence time of the film composition within the homogenous region. As a consequence, the time until phase separation sets in is generally reduced.[42] This in turn suppresses locally delayed phase separation events and thus the formation of finger-like cavities or macrovoids toward the support-facing side of the membrane. This results from an immediate segregation followed by an earlier solidification of the structure across the whole cross-section of the polymer film. As a result, the occurrence of coarsening mechanisms, which lead to the formation of larger voids, is prevented.[42]

When glycerol or acetic acid were added as nonsolvent additives to the casting solution instead of water, similar effects on the morphology could be observed (Figure S1 in the Supporting Information). Although glycerol and acetic acid are in comparison to water less strong nonsolvents, the formation of voids was prevented at similar concentration levels than in case of water. This can be explained by the fact that the use of nonsolvents other than water can lead to a larger heterogeneous region, as it has been observed for other ternary systems.[58,82] As a result, the distance between miscibility gap and composition of the starting solution decreases and less nonsolvent is needed to induce phase separation.[83]

The results, which could be found for the system with NMP were also observed for solutions with 2P as solvent (Figure 4). Similar to the previous case, the formation of macrovoids was suppressed when the amount of nonsolvent within the dope solution was increased. However, there are two main differences between the two solvent systems. On one hand, more water can be added to casting solutions prepared with NMP until the starting composition is close enough to the miscibility gap to cause a suppression of the finger-like morphology. This results from the fact that the miscibility gap for the 2P system is significantly larger than the one of NMP since NMP is a good solvent for PES, whereas 2P is a rather poor solvent.[29] On the other hand, it is striking that the morphology of the sponge-like structure in between the cavities is basically different if comparing the two solvent systems. In particular at high water concentrations, the morphology of the NMP membranes as shown in Figure 2 can rather be regarded as a closed-pore structure. In turn, this can be an indication for a binodal segregation. In contrast, Figure 3 reveals that 2P membranes rather have a lacy structure, which in turn indicates a spinodal segregation followed by a coarsening of the structure. The occurrence of spinodal decomposition in case of 2P can result from a combination of the reduced diffusional exchange and the relatively large overlap of the binodal and the spinodal at low polymer concentrations as it has been shown by Tsai *et al.* for a system with PSf dissolved in 2P.[65] Although the overlap of binodal and spinodal for PSf dissolved in NMP is also relatively large at lower polymer concentrations,[17] the higher diffusional exchange rate may result in a different precipitation path leading to a binodal decomposition.

The differences in the diffusional exchange rates at same solution compositions result from the different dynamic viscosities, which can be observed for the two different solvents. Furthermore, in case of both solvents, the viscosity of the casting solution increased with a rising water concentration (Figure 5).

This can be explained by an increased interaction between the solution components, which are caused by the formation of hydrogen bonds between the molecules.[84,85] The rising viscosity

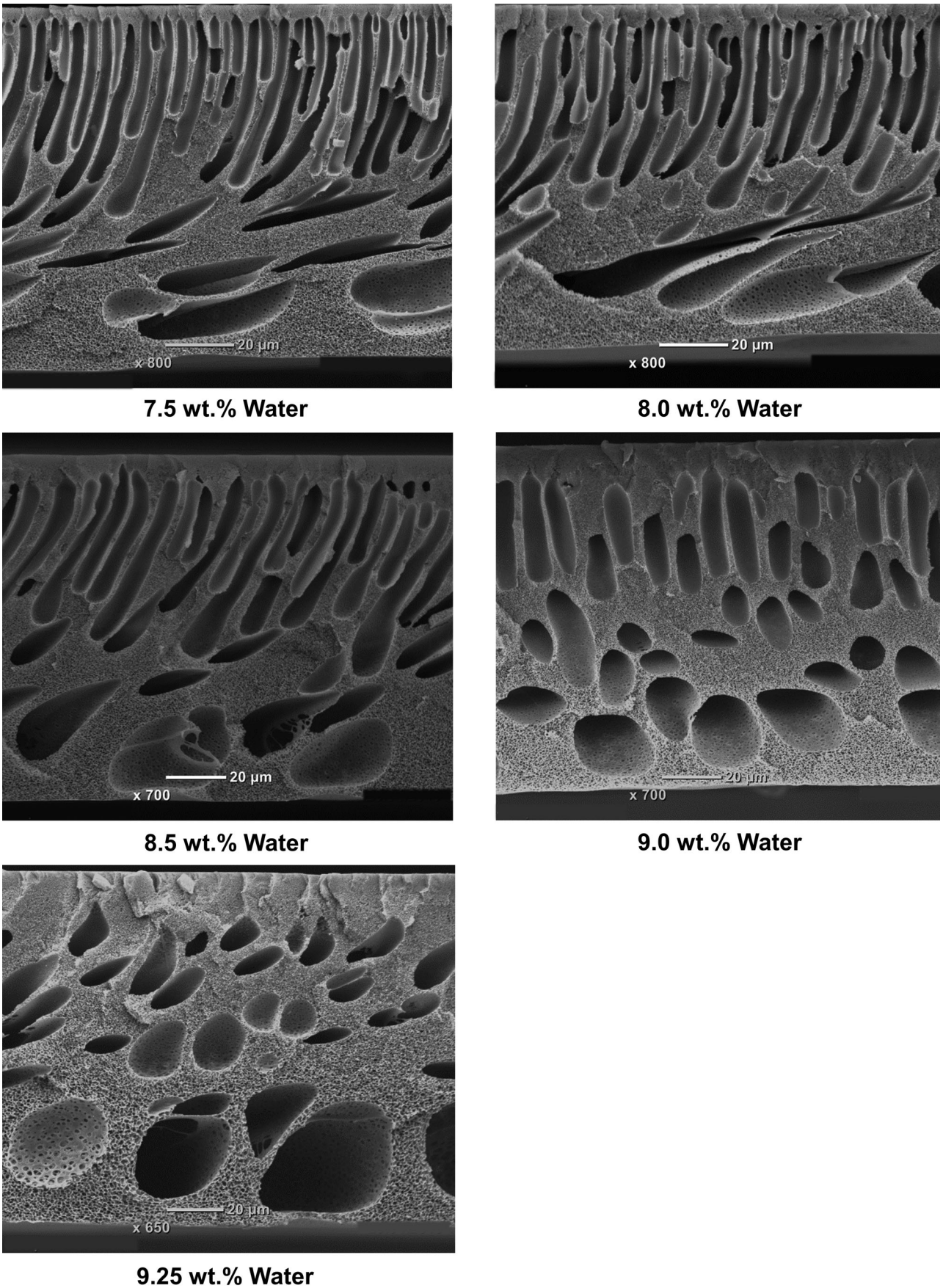

Figure 3. Scanning electron microscopy cross-section images of PES membranes prepared by immersion precipitation with water tempered to 20 °C as non-solvent, where the polymer dope solutions were prepared with 16.88 wt% PES, 0.84 wt% PVP, NMP as solvent and water concentrations varying from 7.5 to 9.25 wt% (image recording potential of 12.5 kV).

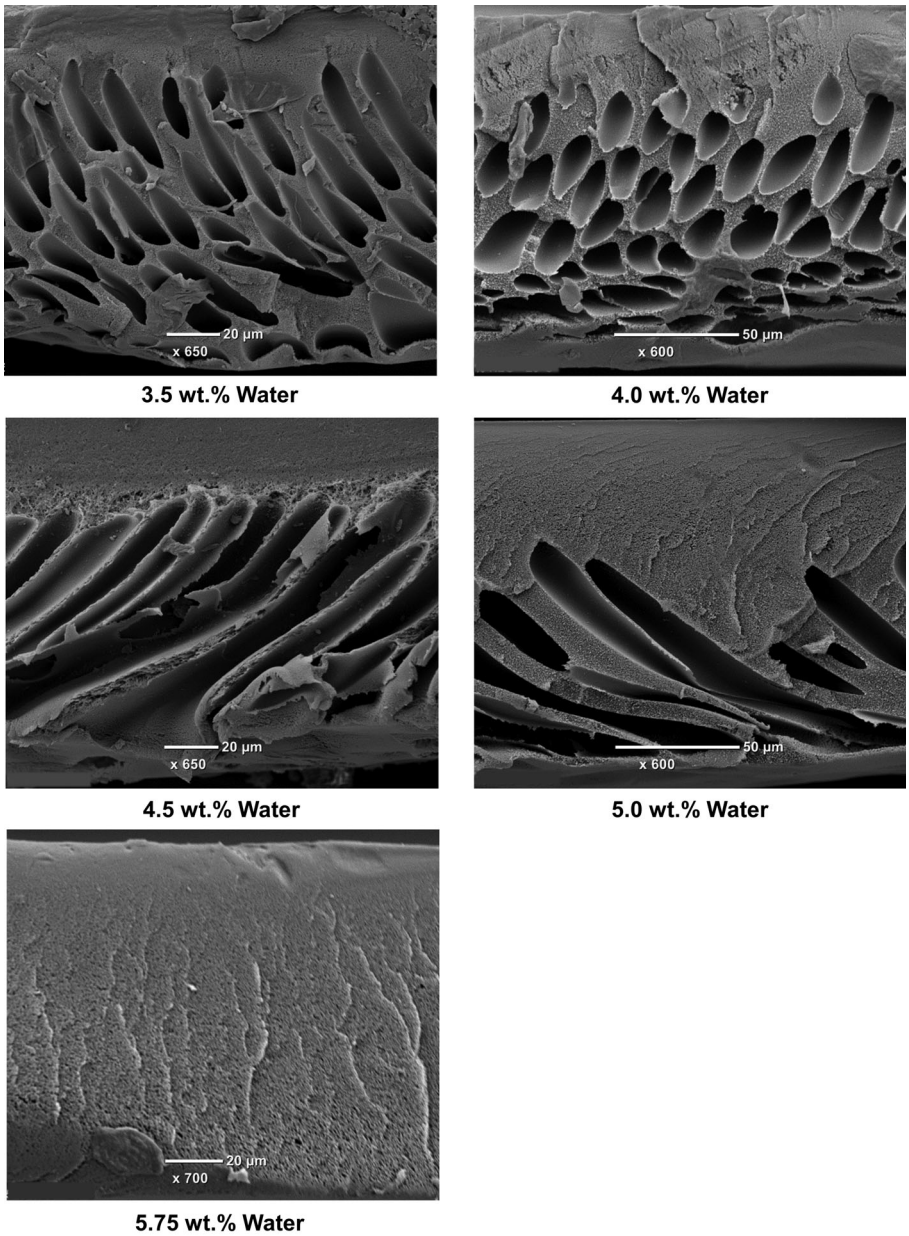

Figure 4. Scanning electron microscopy cross-section images of PES membranes prepared by immersion precipitation with water tempered to 20 °C as nonsolvent, where the polymer dope solutions were prepared with 16.88 wt% PES, 0.84 wt% PVP, 2P as a solvent and water concentrations varying from 3.5 to 5.75 wt% (image recording potential of 12.5 kV).

induces a slowdown of the diffusional exchange between solvent and nonsolvent. As a result, the nuclei of the polymer-poor phase grow with a reduced rate and the formation of macrovoids is suppressed. Ultimately, this effect results in the formation of tighter pore structures.[27,50] Furthermore, the results indicate that the viscosity of the solutions prepared with 2P are about ten times higher than the ones prepared with NMP. On one hand, this can result from the different abilities of the solvents to dissolve PES. It has been previously discussed in the literature that the solvent power has an impact on the viscoelasticity of the resulting solution.[29] On the other hand, 2P has a higher polarity in comparison to NMP.[29] Since the polarity of the solvent can affect the conformation of the polymer, the polarity has an impact on the solution viscosity.[86] Furthermore, the large differences in the solution viscosity would explain why a complete suppression of the finger-like cavities can be achieved when using 2P as solvent. It can be observed in Figure 4 that at water concentrations close to the two phase region a complete sponge-like morphology was obtained in case of membranes prepared with 2P. In contrast, with NMP no complete suppression of macrovoids could be achieved, even if the composition was close to the two phase region (Figure 3). The presence of the finger-like morphology at even higher nonsolvent concentrations can result from the lower viscosity of the polymer solutions, which is not high

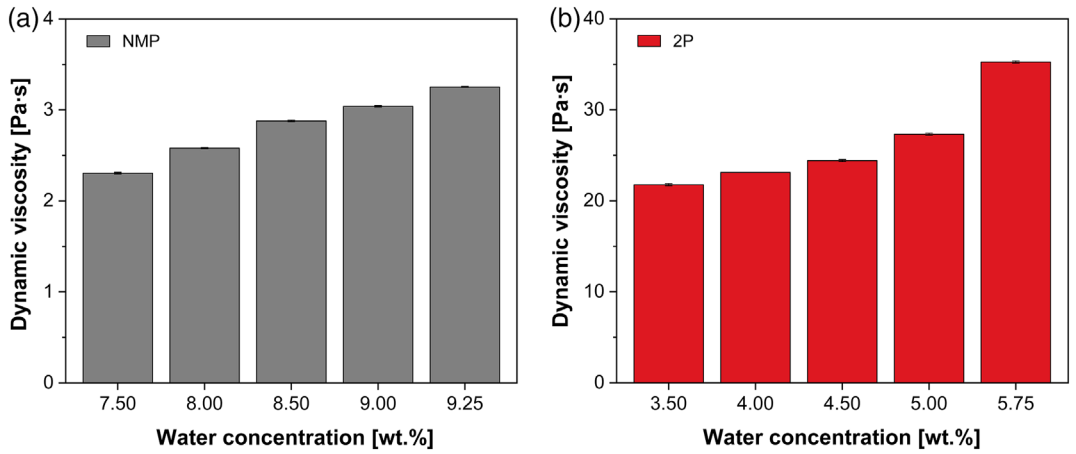

Figure 5. Average dynamic viscosity ± standard deviation (n = 5) in dependence of the water concentration for casting solutions containing 16.88 wt% PES, 0.84 wt% PVP and either NMP (a) or 2P (b) as solvent, determined at 25 °C with a falling ball viscometer. [Color figure can be viewed at wileyonlinelibrary.com]

enough to completely hinder the mechanisms responsible for macrovoid formation such as coalescence and other growth mechanisms.[87]

The pore morphology of the membrane matrix, which is adjacent to the macrovoids, is remarkably different for between the membranes prepared with different solvents. As shown in Figure 6, in case of both solvents the pore size within the sponge-like structure increases the closer it is located toward the support-facing side of the membrane. This can be explained by the greater distance to the precipitation bath and the diffusive resistance, which is caused by the previously formed structures at the air-facing side of the polymer film. As a result, the entry of nonsolvent into the polymer film is slowed down, which in turn extends the time between the onset of phase separation and solidification. In turn, the time for growth and coalescence of the polymer-poor nuclei is prolonged, which ultimately leads to the formation of coarser membrane structures.[25] However, when 2P was used as solvent, the pore size became progressively tighter in the area in which macrovoids are prevalent. This area is indicated by the red arrows in Figure 6. The observation confirms the theory that the growth of the voids is caused by diffusion of the solvent from the surrounding homogenous solution into a nucleus of the polymer-poor phase. As a result of this process, the polymer concentration in the surrounding polymer solution increases. Consequently, this leads to the formation of narrow pores around the voids since the time between onset of phase separation and solidification is reduced by the high polymer concentration. Overall, these results can be attributed to the macrovoid formation mechanism of Smolder and Reuvers, which describes the growth of the voids by solvent diffusion.[42]

Although this phenomenon is not visible for membranes prepared with NMP (Figure 6), it can be assumed that the same mechanism occurs during the structure formation of NMP membranes. However, the effect is not obvious such as in case of 2P due to the open-cellular structure.

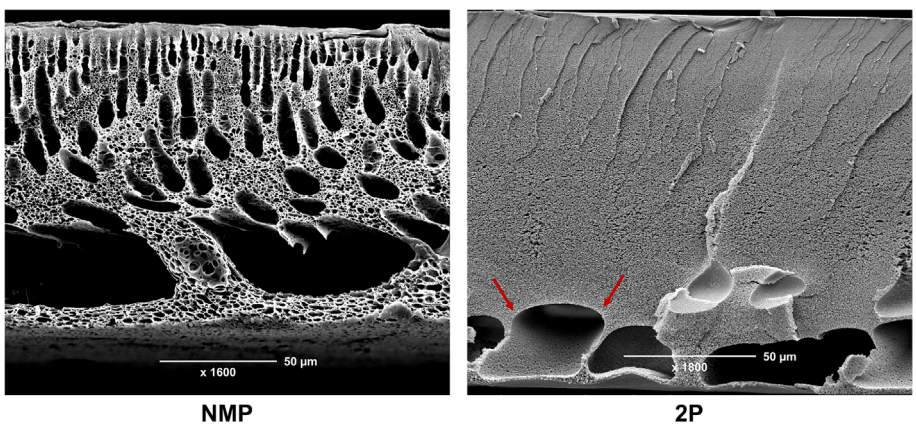

Figure 6. Scanning electron microscopy cross-section images focusing the pore size morphology around the macrovoids of PES membranes prepared by immersion precipitation with water tempered to 40 °C, where the dope solutions were prepared with 16.88 wt% PES, 0.84 wt% PVP, 2.5 wt% glycerol, and either 7.5 wt% water for NMP or 3.5 wt% water for 2P as solvent (image recording potential of 12.5 kV; the red arrows indicate a solvent diffusion-based pore size gradient in case of 2P). [Color figure can be viewed at wileyonlinelibrary.com]

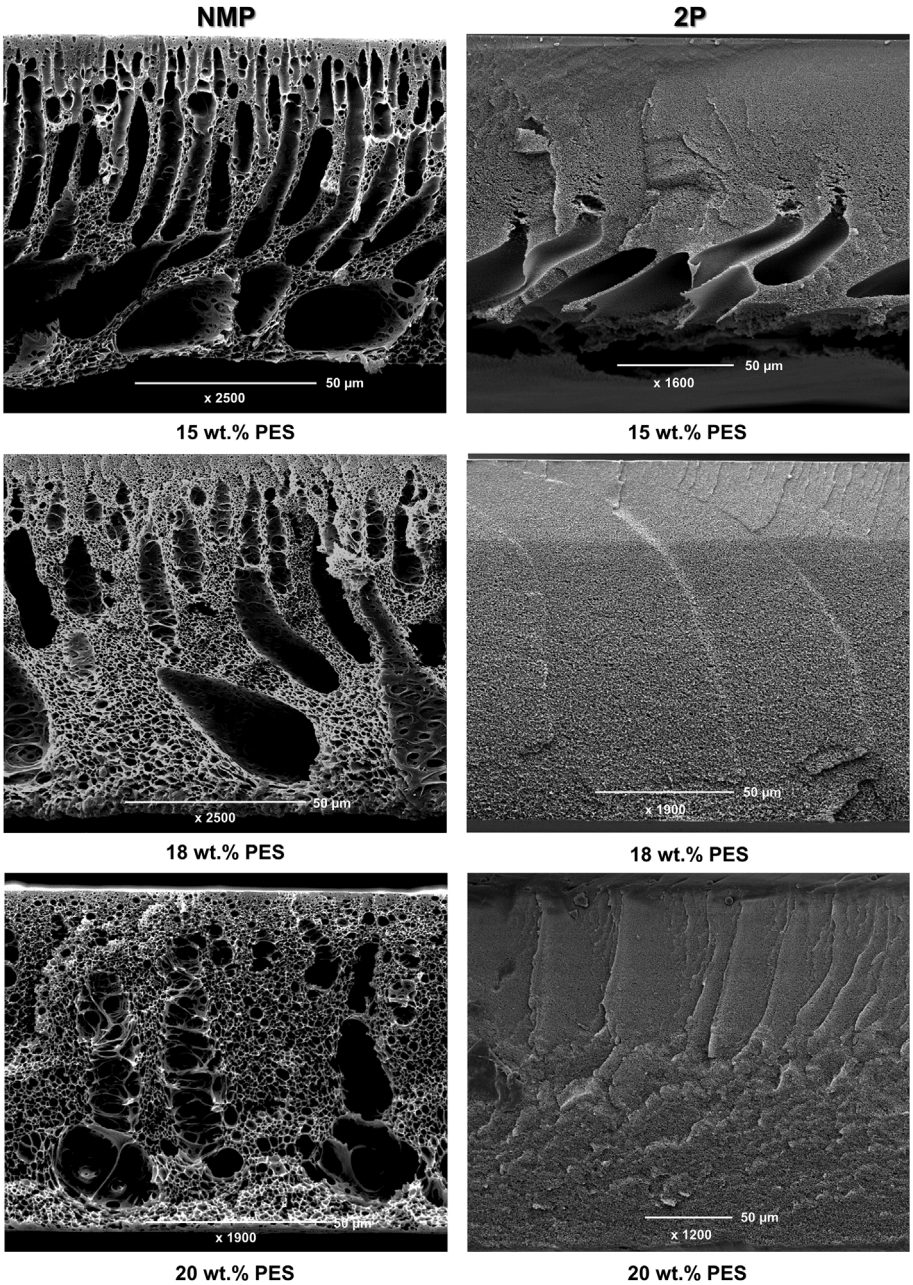

Figure 7. Scanning electron microscopy cross-section images of PES membranes prepared by immersion precipitation with water tempered to 20 °C as non-solvent, where the polymer dope solutions were prepared with PES concentrations varying from 15 to 20 wt%, 0.84 wt% PVP and either 9.0 wt% water in case of NMP or 5.0 wt% water in case of 2P as solvent (image recording potential of 12.5 kV).

Control of the Morphological Structure by Polymer Concentration

Another factor, which leads to a structural transition is the concentration of the membrane-forming polymer within the casting solution. In case of both solvents, a reduction of the macrovoids could be observed when the PES concentration was increased (Figure 7).

In case of NMP, the number and the size of macrovoids visibly decreased when the polymer concentration was raised from 15 to 20 wt%. A similar trend has previously been described for a system with dimethylacetamide (DMAc) and PSf. However, within the same study the investigation of PSf concentration variations with NMP as solvent did not show a clear effect, which is contradictory to the observations made in this study.[23] In contrast, a complete sponge-like morphology could already be obtained at a medium PES concentration when 2P was applied as the solvent. If the PES concentration was further increased to 20 wt%, the sponge-like pore structure became even denser in comparison to the structure obtained with an intermediate concentration. Similar results for both, NMP and 2P, have been published for a system with PSf as the membrane-forming polymer.[40] The effects on the membrane morphology can be explained by the significant increase

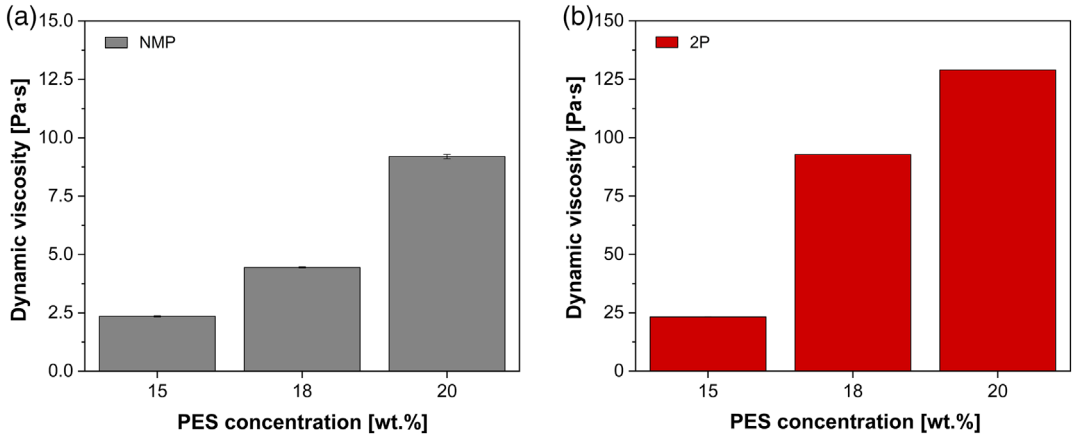

Figure 8. Average dynamic viscosity ± standard deviation (n = 5) in dependence of the PES concentration for casting solutions containing 0.84 wt% PVP and either 9.0 wt% water in case of NMP (a) or 5.0 wt% water in case of 2P (b) as solvent, determined at 25 °C with a falling ball viscometer. [Color figure can be viewed at wileyonlinelibrary.com]

of the viscosity has been found for both solvent systems when the PES concentration was raised (Figure 8).

As a result of the enhanced viscosity, the growth of the nuclei, which are responsible for the development of the macrovoids, is hindered. This is caused by the slowdown of the diffusional exchange of solvent and nonsolvent as well as by the general decrease of the mass transfer processes during structure formation.[39]

Apart from the significant effect on the viscosity, it was found that an elevation of the polymer concentration increases the volume fraction of the polymer matrix. This can be derived from the results of the mechanical stability, which was determined by measurements of the bursting pressure. It was found that the stability of the membranes increased when more PES was added to the membrane casting solution (Figure 9).

Based on the model concept described by Smolders and Reuvers, the observed results can be explained by two opposing effects, which are mainly responsible for the formation of the membrane morphology.[42] On one hand, the increasing polymer concentration at the interface between the polymer film and the precipitation bath provokes the formation of a dense skin layer, which is responsible for the selective separation of molecules. Consequently, this layer acts as an increased diffusion barrier at the air-facing side of the membrane. In turn, this increases the probability that the polymer solution in the lower part of the film remains stable after immersion into the precipitation bath. Therefore, the time until solidification is achieved is prolonged and the formation of finger-like structures is promoted. On the other hand, the phase diagrams of the two systems indicate that with an increase of polymer concentration within the casting solution a smaller amount of water is sufficient to induce phase separation (Figure 2).[29,88] Therefore, it can be assumed that the precipitation process is proceeding quickly so that a locally delayed segregation and solidification is suppressed, resulting in a uniform sponge-like morphology. As it was found that the sponge-like morphology predominates when the polymer concentration is raised, it

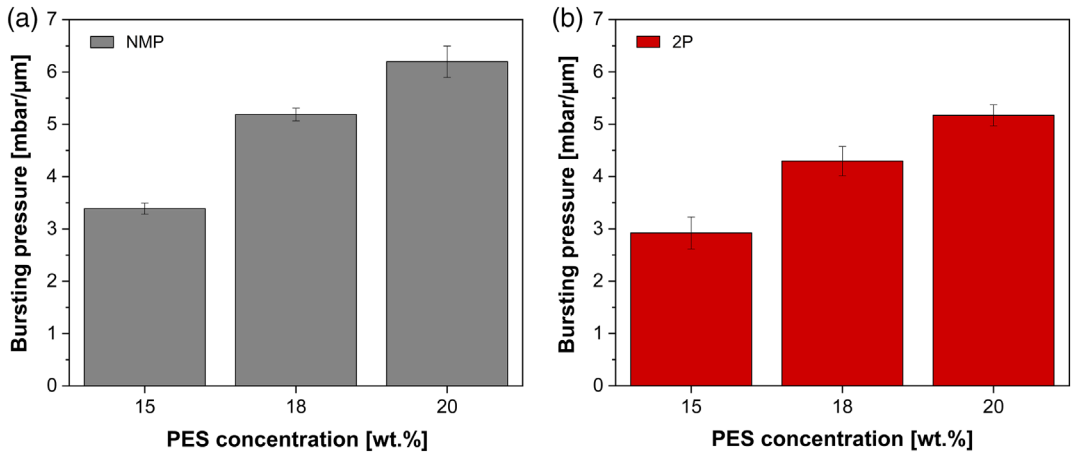

Figure 9. Average bursting pressure normalized to the membrane thickness ± standard deviation (n = 3) in dependence of the PES concentration for membrane prototypes prepared from casting solutions containing 0.84 wt% PVP and either 9.0 wt% water in case of NMP (a) or 5.0 wt% water in case of 2P (b) as solvent. [Color figure can be viewed at wileyonlinelibrary.com]

can be concluded that the second effect overcomes the first on when a certain polymer concentration is reached. A similar relationship between the precipitation rate and the resulting membrane morphology were reported by Smolder and Reuvers.[42] Their investigation of the precipitation rate in a CA/dioxane/water system showed that at a higher polymer content in the casting solution a higher amount of solvent in the precipitation is needed to induce the formation of finger-like structures. Since the share of solvent in the casting solution is reduced with an increase in the polymer concentration, less solvent can diffuse into the precipitation bath. Consequently, a macrovoid-free structure is favored when the polymer concentration is raised. The presence of less solvent in the precipitation bath is additionally enhanced through the decelerated diffusion rate resulting from an increase in viscosity at raised polymer amounts in the casting film. As the result, which were found by Smolders and Reuvers are similar to the observations of this study, the mechanisms caused by an increase of the polymer concentration seem to be independent of the polymer and solvent, which are used for membrane preparation.

Control of the Morphological Structure by Precipitation Conditions

Another possibility to control the membrane structure is the choice of the precipitation medium and the precipitation bath temperature, since both factors influence the mass transfer during the membrane formation process. In general, precipitants with a high affinity toward the solvent promote a fast phase separation process. In contrast, precipitants with a low affinity toward the solvent retard the time between onset of phase separation and solidification of the structure. In order to control the precipitation rate, alcohols have previously been used instead of pure water for ternary systems involving other solvents and membrane-forming polymers than those used in this study.[56,58] Furthermore, it has previously been shown that the precipitation temperature has an impact on the membrane properties due to its effects on both, the rate of diffusion and the viscosity of the casting film within the precipitation bath.[10,26,57,59] However, all these studies only focus on one distinct solvent system. Therefore, until now no comparative study has been conducted, which investigates the effect of the coagulation bath temperature in dependence of the applied solvents including distinct solvent affinities toward the polymer.

This is why the influence of the precipitation conditions on the membrane structure was investigated by comparing the temperature of pure RO-water as precipitant between 20 and 40 °C for membranes prepared with both, NMP and 2P. Additionally, isopropanol was used as an alternative precipitating agent for membrane preparation with both solvents, which exhibit different affinities toward the polymer and the nonsolvent, respectively. The structural results for each precipitation condition and each solvent, respectively, are depicted in Figure 10.

The cross-section images show that the membrane morphology is dependent on the precipitation temperature. When the temperature was set to 20 °C, the morphology was found to consist of a mixture of finger-like and sponge-like structures. While the region of finger-like structures dominated in case of NMP membranes, the sponge-like morphology was found to be prevalent when 2P was applied as a solvent. When the precipitation temperature was raised to 40 °C, however, it could be observed for both solvents that the number of the voids increased. This can be explained by the effect of the temperature on the viscosity of the polymer film. When the temperature of the precipitation bath is increased, the viscosity of the casting film decreases and at the same time the diffusion rate of solvent and nonsolvent increases.[57] As a consequence of the increased diffusion speed, the solvent uptake is enhanced, which results in an increased growth of the polymer-poor nuclei. This in turn promotes the development of voids and the formation of open pore structures.[33] In contrast, at low precipitation temperatures, the growth of the nuclei is inhibited. Consequently, new nuclei can form below the already existing ones so that the formation of the macrovoids is suppressed. A similar effect has been reported for a system consisting of cellulose acetate in NMP.[89] Furthermore, it would be expected that the temperature has an effect on the thermodynamics of the system and therefore affects the resulting membrane structure. However, it has been previously shown, that the location of the miscibility gap for the systems examined in this study is not affected by the temperature at which phase separation takes place.[88] Therefore, the effect of the temperature on the thermodynamics and its influence on the membrane structure is negligible.

When isopropanol was used instead of water as the precipitating agent, it could be clearly observed that the turbidity of the polymer film increased significantly slower in case of isopropanol during the precipitation process. This results from the lower precipitation rate when using isopropanol, which consequently causes a delayed precipitation of the film.[90] Since the exchange of solvent and nonsolvent proceeds more equally across the entire polymer solution profile, the formation of nuclei occurs almost simultaneously at every position within the film. In turn, this reduces the probability for the development of finger-like structures. Although in case of both solvents, a few voids were still present in the substructure of the membrane cross-section, in comparison to the precipitation at the same temperature with water, the number and size of the voids visibly decreased for membranes prepared with isopropanol as nonsolvent.

Control of the Membrane Performance by Non-Solvent Additives

The addition of nonsolvent additives to the casting solution does not only influence the morphology of the membrane but it has also an impact on the membrane permeability and its retention capacity. In dependence of the applied solvent, two different behaviors could be observed if water was added to the polymer solution (Figure 11). When NMP was applied for the preparation of the casting solutions, the permeability increased with a raising amount of water within the solution. At a concentration of 8.5 wt % water, however, the permeability reached a maximum and started to decrease with a further addition of water to the casting solution. At the same time, the retention of lysozyme exhibited an inversely proportional behavior. It declined with raising water concentrations in the casting solution until an amount of 8.5 wt % water was reached, and started to increase again when the water share within the polymer solution was further increased.

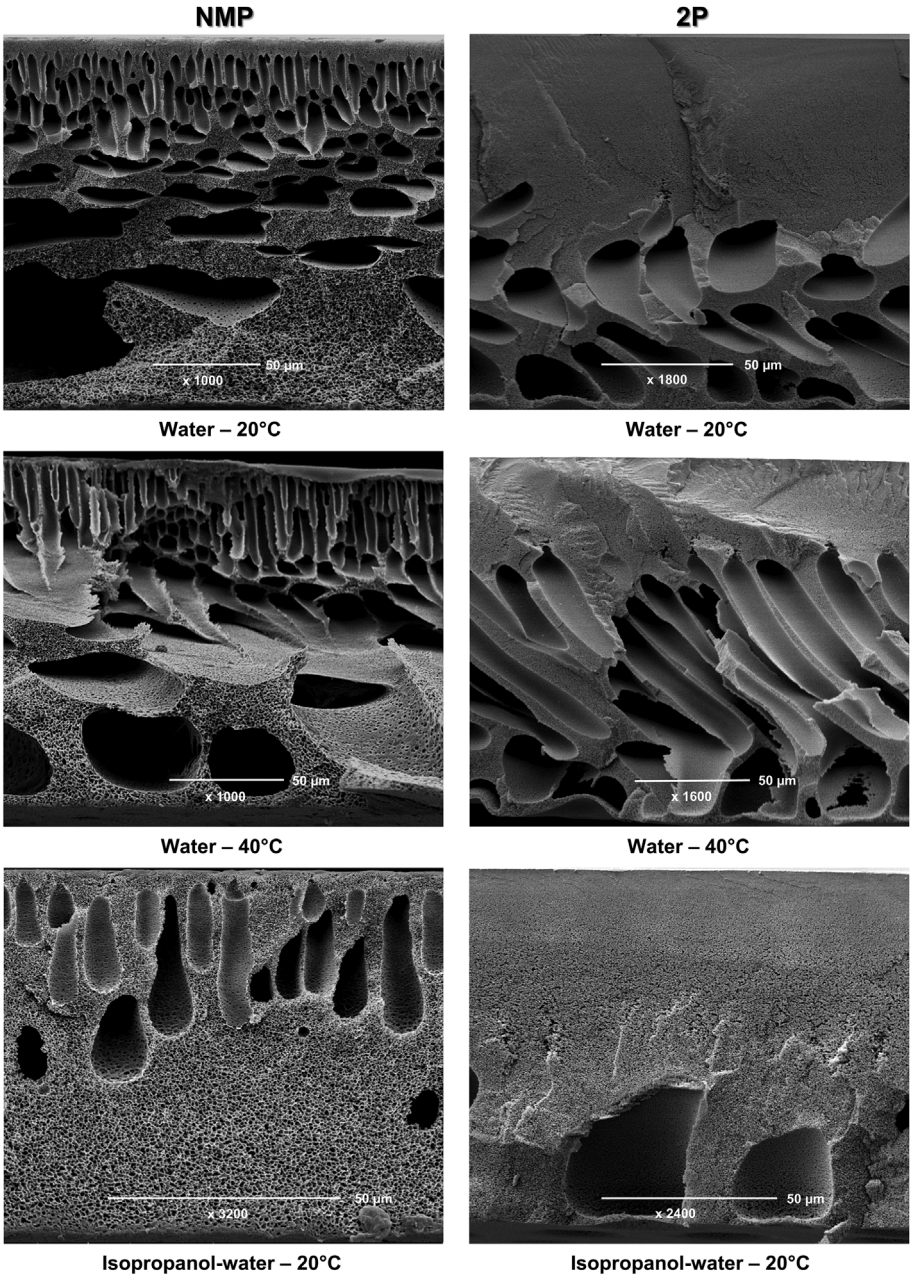

Figure 10. Scanning electron microscopy crosssection images of PES membranes prepared by immersion precipitation at different precipitation temperatures and with different precipitating agents, where the polymer dope solutions were prepared with 16.88 wt% PES, 0.84 wt% PVP, and either 7.5 wt% water in case of NMP or 3.5 wt% water in case of 2P as solvent (image recording potential of 12.5 kV).

However, the changes in lysozyme retention are rather small. In contrast, the permeability of 2P membranes did not show a clear trend in dependence on the water concentration. It rather fluctuated around a value of 200 $L/m^2 \cdot h \cdot bar$. Nonetheless, a clear trend could be observed for the lysozyme retention as it continuously decreased when the water concentration was raised.

Similar trends for permeability and lysozyme retention were found when glycerol was applied as nonsolvent instead of water (Figure 12). In case of NMP, the permeability raised and exhibited a maximum at 2.5 wt% glycerol whereas it decreased when the concentration was further raised to 5 wt%. In contrast to the water variation, the retention slightly increased with an addition of 2.5 wt% glycerol and stayed at the same level when the concentration was further increased 5 wt%. However, the effect on the retention again was rather small. In contrast, the permeability constantly raised with an increase of glycerol in the dope solution, if 2P was applied as solvent. At the same time, the lysozyme retention exhibited an inversely proportional behavior and declined with raising glycerol concentrations.

When 2P was applied as a solvent and acetic acid was added as nonsolvent to the polymer solution, the same observations were made as in case of the glycerol variations (Figure 12). While the

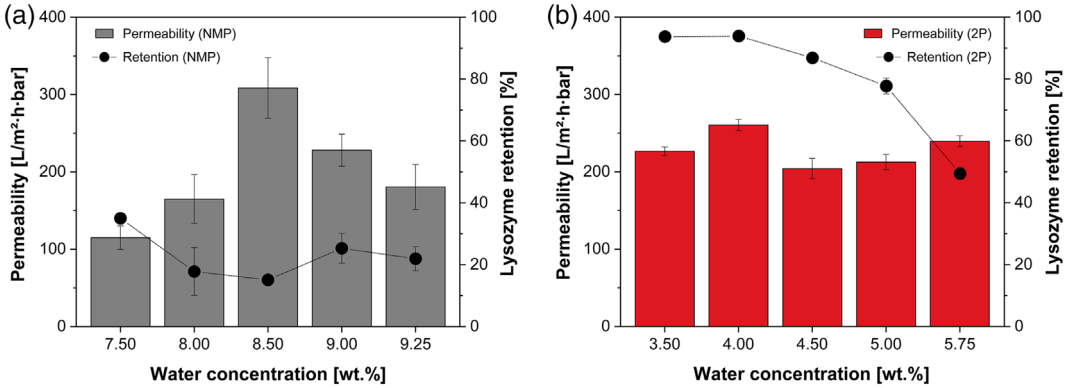

Figure 11. Average membrane permeability and respective lysozyme retention ± standard deviation (n = 3) in dependence of the water concentration for membrane prototypes prepared with water tempered to 20 °C from casting solutions containing 16.88 wt% PES, 0.84 wt% PVP and either NMP (a) or 2P (b) as solvent. [Color figure can be viewed at wileyonlinelibrary.com]

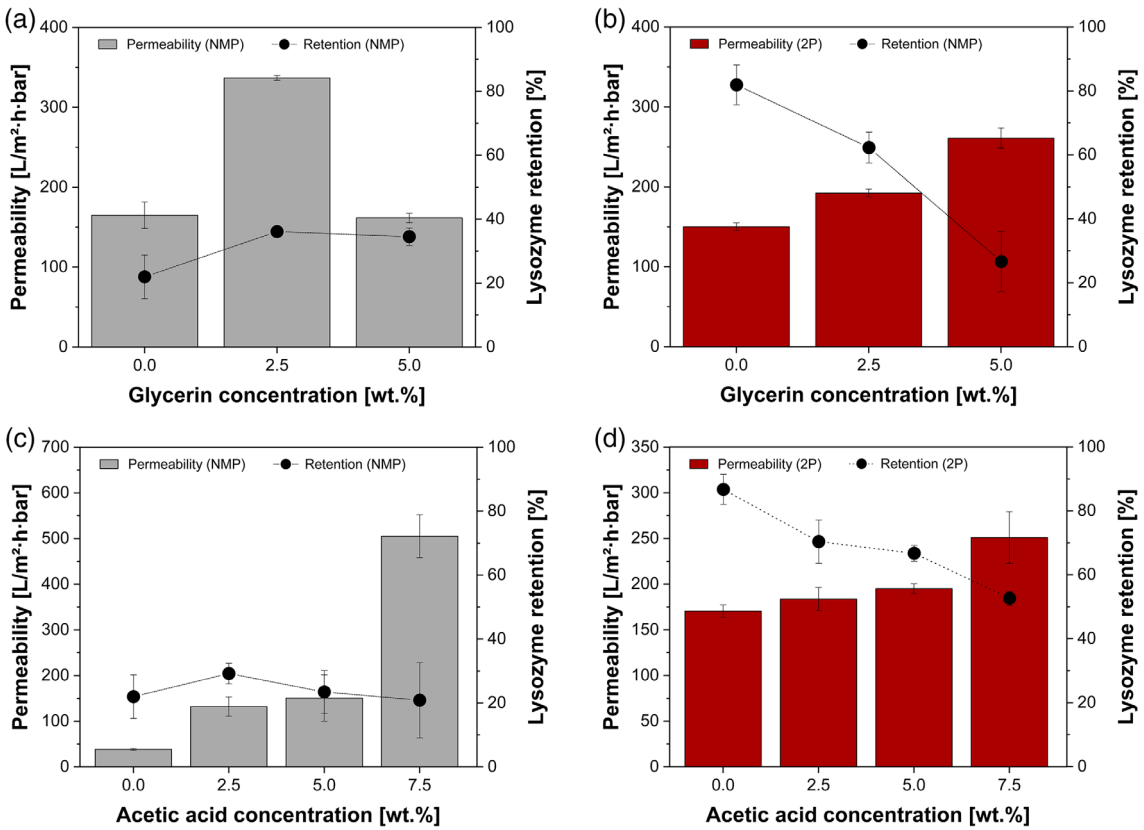

Figure 12. Average membrane permeability and the respective lysozyme retention ± standard deviation (n = 3) in dependence of the glycerol concentration for membrane prototypes prepared with water tempered to 20 °C from casting solutions containing 16.88 wt% PES, 0.84 wt% PVP, and either 7.5 wt% water in case of NMP (a) or 3.5 wt% water in case of 2P (b) as solvent, as well as in dependence of the acetic acid concentration for membrane prototypes prepared from casting solutions containing 16.88 wt% PES, 0.84 wt% PVP, and either 7.5 wt% water in case of NMP (c) or 3.5 wt% in case of 2P (d) as solvent. [Color figure can be viewed at wileyonlinelibrary.com]

permeability constantly increased with a raise in the acetic acid concentration, the lysozyme retention decreased inversely proportional. In contrast, the behavior for NMP membranes was slightly different. The permeability continuously increased with a raising acetic acid concentration. However, the lysozyme retention was not significantly influenced by changes in the acetic acid amount since it constantly fluctuates around 20%.

The increase of the permeability, which was partially observed for the different variation series, has also been reported for other ternary systems. Chaturvedi *et al.* for instance varied the proportions of maleic acid (nonsolvent) and dimethylformamide (solvent), while the PES concentration was at the same time held at a constant level. They found that an increase of the maleic acid concentration results in an linearly raising water permeability.[91]

On one hand, the morphology results indicate that the thickness of the sponge-like layer is strongly influenced by the content of nonsolvent within the casting solution (Figures 3 and 4). Since the sponge-like proportions significantly contribute to the flow resistance of the membrane, it also has an impact on the permeability of the membrane. On the other hand, the impact of nonsolvents on the membrane performance can be explained by two contrary effects, which influence the position of the dope solution composition within the phase diagram, and therefore the entry point into the miscibility gap. The effects have been explained by Wijmans.[92] In general, the original position of the dope solution is shifted toward the miscibility gap when the nonsolvent concentration is raised, while the polymer concentration at the same time remains constant. Consequently, the starting phase separation leads to lower polymer concentrations in the polymer-rich phase so that more open pore structures result from an increasing nonsolvent concentration in the dope solution. On the other hand, the exchange ratio of solvent and nonsolvent cannot be considered to remain constant. As the content of nonsolvent increases, the ratio between the inflow of nonsolvent and the export of solvent from the casting film declines, because with respect to the nonsolvent the chemical potential between the casting film and the precipitation bath is reduced. In comparison, a higher level of nonsolvent leads to an increased export of solvent from the casting film, which causes a steeper entry into the miscibility (refer to Figure S2 in the supporting information). This in turn would lead to an open pore structure since the entry into the heterogeneous region shifts toward lower polymer concentrations with a raising amount of nonsolvent.

Therefore, an overall prediction of the effect on the pore sizes caused by an increasing nonsolvent amount in the dope solution is not possible. However, for the 2P system the shift of the initial dope solution composition toward the miscibility gap seems to superimpose the influence on the mass transfer ratio. Similarly, the effect caused by the location of the initial composition also seems to superimpose the second effect in case of NMP, until a concentration of 8.5 wt% is reached. When the amount of nonsolvent is further increased, however, this effect is exceeded by the change in the mass transfer ratio. As a consequence, the permeability starts to decrease with a further raise of the nonsolvent amount in the dope solution. An exception for this behavior could be observed for the acetic acid variations in NMP. In this case, a continuous increase of the permeability was found when the acetic acid concentration was raised. As in case of 2P, this can be explained by the effect caused through the shift of the initial solution composition toward the miscibility gap, which overweighs the effect on the mass transfer ratio over the entire investigated concentration range. The different behavior in contrast to water and glycerol variations in NMP can be related to the strength of the nonsolvent. While water is a very strong nonsolvent for PES, acetic acid is a rather week nonsolvent for this polymer. Therefore, the balance of both effects shifts in dependence of the nonsolvent strength, which would explain the different trends.

Control of the Membrane Performance by Polymer Concentration

Apart from the mechanical stability of the membrane, the concentration of the membrane-forming polymer generally influences the overall porosity and the pore sizes of the membrane.[7] Therefore both, permeability and protein retention, are affected by changes in the polymer concentration. Independent of the solvent, which was applied, a decline of the permeability could be observed when the PES concentration was raised. Inversely proportional to the permeability, the lysozyme retention increased with a raising PES concentration (Figure 13).

A similar tendency has already been reported for polysulfone dissolved in a mixture of NMP and tetrahydrofuran,[24] which confirms that the influence of the polymer concentration is completely independent of the applied solvent. The impact of the polymer concentration on the membrane features can be explained on the basis of the phase diagram. If it is assumed that the influence of the polymer concentration on the mass transfer ratio of nonsolvent and solvent is negligible, the slope of the entry path into the heterogeneous region remains identical, regardless of the polymer concentration in the dope solution.[92] Therefore, the composition at the entry point into the miscibility gap is strongly influenced by the initial polymer concentration (refer to Figure S3 of the supporting information). If the initial composition is located at a higher polymer concentration, the proportion of solvent within the polymer-poor phase is reduced after onset of the phase separation. In turn, the nascent pore size

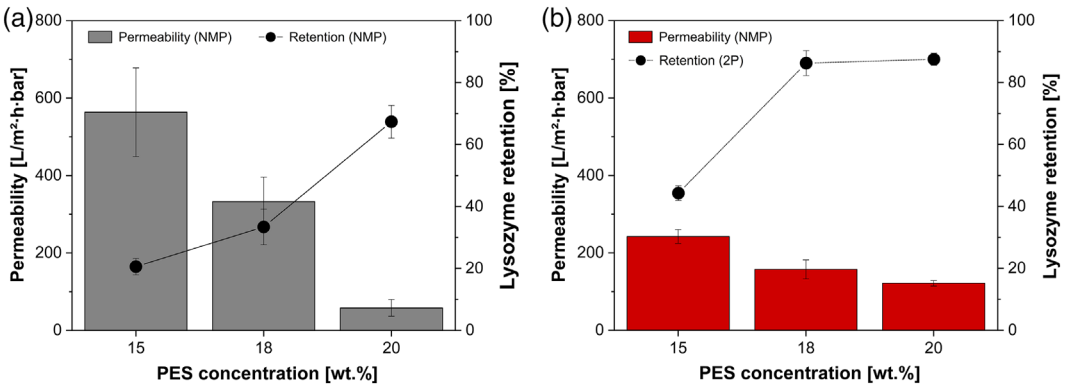

Figure 13. Average membrane permeability and the respective lysozyme retention ± standard deviation (n = 3) in dependence of the PES concentration for membrane prototypes prepared with water tempered to 20 °C from casting solutions additionally containing 0.84 wt% PVP and 9.0 wt% water in case of NMP (a) or 5.0 wt% water in case of 2P (b) as solvent. [Color figure can be viewed at wileyonlinelibrary.com]

after phase separation is significantly influenced. Due to the thermodynamic equilibrium between the two forming phases, the polymer-rich phase consequently consists of a higher polymer content. This in turn results in a higher amount of polymer within the membrane matrix and therefore in a decreased permeability on one hand, and an increased protein retention on the other hand.

Control of the Membrane Performance by Precipitation Conditions

It has been shown earlier that the membrane structure is visibly influenced by the precipitation conditions. Since membrane performance and structure are closely related to each other, the membrane performance was also found to be influenced by a change of the conditions within the precipitation bath. It could be observed that an increase of the water temperature in the precipitation bath resulted in a decreased permeability for membranes prepared with NMP, whereas the permeability of 2P membranes was significantly increased (Figure 14). When the water in the precipitation bath was displaced by isopropanol as a weaker nonsolvent for PES, the permeability increased independently of the solvent, which was applied. In all cases, the observed changes in the lysozyme retention were inversely proportional to the changes in the permeability.

In case of 2P, the observed permeability increase at a higher precipitation temperature can be explained by two effects. On one hand, the increasing temperature accelerates the diffusive exchange between nonsolvent and solvent. On the other hand, the viscosity of the casting solution film is reduced when the temperature is raised, which in turn also accelerates the mass transfer between casting film and precipitation bath.[58] Consequently, the nuclei of the polymer-poor phase can grow more quickly so that larger pores are formed. This in turn causes an increase in permeability and a simultaneous decrease in the lysozyme retention.

In case of NMP a similar effect would be expected, since due to the two described effects the pore structure is expected to become more open, which in turn increases the permeability. However, against the expectations it was found that the permeability slightly decreased when the precipitation temperature was raised, whereas the retention in contrast slightly increased. Although this increase cannot be regarded to be significant, the observed differences between the two solvent systems can be explained by the different formation mechanisms, which dominate depending on the respective solvent type. While the lacy structures of the 2P membranes indicate that these membranes were formed through a spinodal decomposition, which is followed by a subsequent coarsening of the structures, the structure of the NMP membranes can be described as a closed-cellular structure. On one hand, the combination of the increased water content and the higher precipitation temperature results in an instantaneous entry into the two-phase region when the casting film is immersed into the precipitation bath. On the other hand, the enhanced diffusion rate caused by the temperature increase leads to a higher rate of coalescence with respect to the polymer-poor phase. Although this should lead to the formation of coarser structures, the overall number of pores decreases in case of NMP membranes due to the formation of a closed-cellular structure. As a result, the reduction of the pore quantity and the thereby caused decrease in permeable pores finally leads to a decline in permeability. Since the closed-cellular structure of the NMP membranes in comparison to the lacy structure of the 2P membranes affects the flow-retention ratio in an undesired manner, there was found hardly any difference between the lysozyme retention for NMP membranes prepared at 20 or 40 °C.

When isopropanol was used for membrane fabrication at a constant precipitation temperature of 20 °C instead of water, the permeability increased and the lysozyme retention decreased independent of the solvent which was used. As already mentioned, the addition of isopropanol leads to a reduction of the precipitation rate, which in turn prolongs the duration between the onset of phase separation and the solidification of the structure.[90] Consequently, this enables a coarsening of the pore structure through growth and coalescence, which in turn results in an increase in membrane permeability. The opposite effect of isopropanol precipitation in comparison to a change in the water bath temperature can be explained by the phase diagram of the respective system. It has been previously shown for a system of

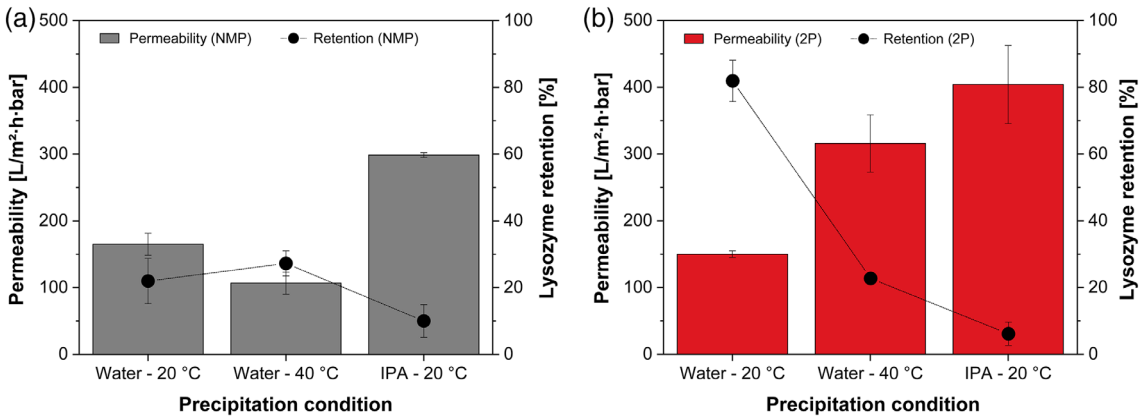

Figure 14. Average membrane permeability and the respective lysozyme retention ± standard deviation (n = 3) in dependence of the precipitation bath conditions for the fabrication of membrane prototypes prepared with different nonsolvents at different temperatures from casting solutions containing 16.88 wt % PES, 0.84 wt% PVP, and either 7.5 wt% water in case of NMP (a) or 3.5 wt% water in case of 2P (b) as solvent. [Color figure can be viewed at wileyonlinelibrary.com]

NMP, PES, and water that the temperature has no visible influence on the location of the two-phase region.[88] However, the addition of isopropanol results in a shift of the miscibility gap, as its addition expands the ternary system consisting of water, solvent and PES to a four component system consisting of water, isopropanol, the solvent, and PES. Since isopropanol is a weaker solvent than water, the size of the miscibility gap decreases, which has been shown for other systems such as for PES in DMSO.[66,93] As a result, the phase separation in isopropanol is introduced at a later point of time in comparison to a precipitation in pure water. Furthermore, the ratio of polymer, solvent and nonsolvent in the developing phases is affected, which can also contribute to the observed increase in permeability and the slight decrease in retention.

CONCLUSIONS

This work presents a comparative study of PES membrane formation via nonsolvent induced phase separation between two different polymeric systems using NMP as conventional solvent and 2P as a greener alternative for the preparation of the dope solutions. In this context, a comprehensive investigation on the effects of the polymer concentration, the choice of the nonsolvent additives, and the precipitation conditions was performed in both solvent systems, NMP and 2P, respectively. The effects of the variables were studied with regard to the formation of the structure on one hand, and regarding the performance of the resulting membrane prototypes on the other hand. It was found that the general structure differs between the two solvent systems. NMP membranes exhibited a closed-cellular structure, while the membranes prepared with 2P exhibited a lacy structure. It was found that the addition of different nonsolvents to the dope solutions, the application of lower precipitation temperatures and weaker nonsolvents in the precipitation bath as well as the increase of the polymer concentration suppressed the formation of finger-like structures and macrovoids. The effects on the morphological cross-section features were observed for all systems, regardless of the solvent, which was applied for dope solution preparation. In contrast, the effects on the performance of the membranes partially differed in dependence on the applied solvent system. While an increasing polymer concentration in both solution systems resulted in a decrease in permeability and a simultaneous increase in retention, the influences of nonsolvent addition and precipitation conditions on membrane performance in certain cases differed in dependence of the applied solvent. It could be shown that the addition of nonsolvent to 2P dope solutions results in an increase in permeability and an inversely correlating decrease in the lysozyme retention. In contrast to these findings, with an exception of acetic acid variations, the prototypes produced with NMP exhibited a maximum at a certain nonsolvent concentration in the solution. When the concentration was further raised, the permeability started decreasing again. However, the lysozyme retention was also in all cases negatively proportional to the permeability, although the effects on the retention were less pronounced than in case of 2P membranes. Furthermore, the increase of the precipitation temperature resulted in an increased permeability and a decreased retention for 2P membranes, whereas the permeability declined and the retention increased when the same precipitation conditions were applied for membrane fabrication using NMP. The results can be explained by the different thermodynamic and kinetic features of the formation process, which are strongly related to the applied solvent system. While the dominating formation mechanism in case of NMP is assumed to be a binodal decomposition, 2P membranes result from a spinodal decomposition. Both formation mechanisms are differently influenced by the tested variables and therefore result in different outcomes on structure and performance in dependence of the applied solvent.

ACKNOWLEDGMENTS

The authors would like to thank Heike Hepprich from the Sartorius membrane development team for the recording of the SEM crosssection images, as well as Pascal Kircher for his assistance in performing the experiments.

REFERENCES

1. Baker, R. W. Membrane Technology and Applications; John Wiley & Sons, Ltd.: Chichester, UK, **2012**.
2. Wickramasinghe, S. R.; Stump, E. D.; Grzenia, D. L.; Husson, S. M.; Pellegrino, J. *J. Membr. Sci.* **2010**, *365*, 160.
3. Fang, X.; Li, J.; Li, X.; Sun, X.; Shen, J.; Han, W.; Wang, L. *J. Membr. Sci.* **2015**, *476*, 216.
4. Eren, E.; Sarihan, A.; Eren, B.; Gumus, H.; Kocak, F. O. *J. Membr. Sci.* **2015**, *475*, 1.
5. Tylkowski, B.; Tsibranska, I. *J. Chem. Technol. Metallur.* **2015**, *50*, 3.
6. Strathmann, H. *Food Biotechnol.* **1990**, *4*, 253.
7. Akbari, A.; Yegani, R. *J. Membrane Separation Technol.* **2012**, *1*, 100.
8. Guillen, G. R.; Pan, Y.; Li, M.; Hoek, E. M. V. *Indus. Eng. Chem. Res.* **2011**, *50*, 3798.
9. Strathmann, H.; Kock, K. *Desalination*. **1977**, *21*, 241.
10. Li, J.-F.; Xu, Z.-L.; Yang, H. *Polym. Adv. Technol.* **2008**, *19*, 251.
11. Wang, D.; Li, K.; Sourirajan, S.; Teo, W. K. *J. Appl. Polym. Sci.* **1993**, *50*, 1693.
12. Barzin, J.; Madaeni, S. S.; Mirzadeh, H.; Mehrabzadeh, M. *J. Appl. Polym. Sci.* **2004**, *92*, 3804.
13. Rahimpour, A.; Madaeni, S. S. *J. Membr. Sci.* **2007**, *305*, 299.
14. Arthanareeswaran, G.; Starov, V. M. *Desalination*. **2011**, *267*, 57.
15. Alenazi, N. A.; Hussein, M. A.; Alamry, K. A.; Asiri, A. M. *Desig. Monomers Polym.* **2017**, *20*, 532.
16. Baik, K.-J.; Kim, J. Y.; Lee, H. K.; Kim, S. C. *J. Appl. Polym. Sci.* **1999**, *74*, 2113.
17. Barzin, J.; Sadatnia, B. *Polymer*. **2007**, *48*, 1620.
18. Yi, Z.; Zhu, L.-P.; Xu, Y.-Y.; Zhao, Y.-F.; Ma, X.-T.; Zhu, B.-K. *J. Membr. Sci.* **2010**, *365*, 25.
19. Zhou, C.; Hou, Z.; Lu, X.; Liu, Z.; Bian, X.; Shi, L.; Li, L. *Indus. Eng. Chem. Res.* **2010**, *49*, 9988.
20. Irfan, M.; Idris, A. *Mater. Sci. Eng. C.* **2015**, *56*, 574.

21. Yi, Z.; Zhu, L.-P.; Zhao, Y.-F.; Zhu, B.-K.; Xu, Y.-Y. *J. Membr. Sci.* **2012**, *390-391*, 48.
22. Yilmaz, G.; Toiserkani, H.; Demirkol, D. O.; Sakarya, S.; Timur, S.; Torun, L.; Yagci, Y. *Mater. Sci. Eng. C.* **2011**, *31*, 1091.
23. Barzin, J.; Sadatnia, B. *J. Membr. Sci.* **2008**, *325*, 92.
24. Hołda, A. K.; Vankelecom, I. F. J. *J. Appl. Polym. Sci.* **2015**, *132*, 42130.
25. Astakhov, E. Y.; Zhironkin, S. F.; Kolganov, I. M.; Klinshpont, E. R.; Tsarin, P. G. *Polym. Sci. Series A*. **2011**, *53*, 613.
26. Amirilargani, M.; Saljoughi, E.; Mohammadi, T.; Moghbeli, M. R. *Polym. Eng. Sci.* **2010**, *50*, 885.
27. Saljoughi, E.; Sadrzadeh, M.; Mohammadi, T. *J. Membr. Sci.* **2009**, *326*, 627.
28. Barth, C.; Wolf, B. A. *Macromol. Chem. Phys.* **2000**, *201*, 365.
29. Mousavi, S. M.; Zadhoush, A. *J. Membr. Sci.* **2017**, *532*, 47.
30. Idris, A.; Man, Z.; Maulud, A. S.; Khan, M. S.; Suetsugu, S. *Membranes*. **2017**, *7*, 21.
31. Yu, L.; Yang, F.; Xiang, M. *RSC Adv.* **2014**, *4*, 42391.
32. Chakrabarty, B.; Ghoshal, A. K.; Purkait, M. K. *J. Membr. Sci.* **2008**, *315*, 36.
33. Xu, J.; Tang, Y.; Wang, Y.; Shan, B.; Yu, L.; Gao, C. *J. Membr. Sci.* **2014**, *455*, 121.
34. Ohlrogge, K.; Ebert, K., Eds. Membranen: Grundlagen, Verfahren und industrielle Anwendungen; Wiley-VCH Verlag GmbH & Co. KGaA: Weinheim, Germany, **2006**.
35. Xu, Z.-L.; Alsalhy Qusay, F. *J. Membr. Sci.* **2004**, *233*, 101.
36. Zeman, L. J.; Zydney, A. L. Microfiltration and Ultrafiltration: Principles and Applications; CRC Press: Boca Raton, FL, **1996**.
37. Drioli, E.; Giorno, L.; Fontananova, E., Eds. Comprehensive Membrane Science and Engineering. 2nd ed.; Oxford: Elsevier, **2017**.
38. Feng, Y.; Han, G.; Zhang, L.; Chen, S.-B.; Chung, T.-S.; Weber, M.; Staudt, C.; Maletzko, C. *Polymer*. **2016**, *99*, 72.
39. Guillen, G. R.; Ramon, G. Z.; Kavehpour, H. P.; Kaner, R. B.; Hoek, E. M. V. *J. Membr. Sci.* **2013**, *431*, 212.
40. Hung, W.-L.; Wang, D.-M.; Lai, J.-Y.; Chou, S.-C. *J. Membr. Sci.* **2016**, *505*, 70.
41. Strathmann, H.; Kock, K.; Amar, P.; Baker, R. W. *Desalination*. **1975**, *16*, 179.
42. Smolders, C. A.; Reuvers, A. J.; Boom, R. M.; Wienk, I. M. *J. Membr. Sci.* **1992**, *73*, 259.
43. Prakash, S. S.; Francis, L. F.; Scriven, L. E. *J. Membr. Sci.* **2006**, *283*, 328.
44. Wang, B.; Lai, Z. *J. Membr. Sci.* **2012**, *405-406*, 275.
45. Wang, D.-M.; Lin, F.-C.; Wu, T.-T.; Lai, J.-Y. *J. Membr. Sci.* **1998**, *142*, 191.
46. Kaiser, V.; Stropnik, C. *Acta Chimica Slovenica*. **2000**, *47*, 205.
47. Kim, J. Y.; Kim, Y. D.; Kanamori, T.; Lee, H. K.; Baik, K.-J.; Kim, S. C. *J. Appl. Polym. Sci.* **1999**, *71*, 431.
48. Li, S.-G.; van den Boomgaard, T.; Smolders, C. A.; Strathmann, H. *Macromolecules*. **1996**, *29*, 2053.
49. Wijmans, J. G.; Kant, J.; Mulder, M. H. V.; Smolders, C. A. *Polymer*. **1985**, *26*, 1539.
50. van de Witte, P.; Dijkstra, P. J.; van den Berg, J. W. A.; Feijen, J. *J. Membr. Sci.* **1996**, *117*, 1.
51. Lee, K.-W.; Seo, B.-K.; Nam, S.-T.; Han, M.-J. *Desalination*. **2003**, *159*, 289.
52. Wienk, I. M.; Boom, R. M.; Beerlage, M. A. M.; Bulte, A. M. W.; Smolders, C. A.; Strathmann, H. *J. Membr. Sci.* **1996**, *113*, 361.
53. Sadrzadeh, M.; Bhattacharjee, S. *J. Membr. Sci.* **2013**, *441*, 31.
54. Barton, B. F.; Reeve, J. L.; McHugh, A. J. *J Polym Sci B*. **1997**, *35*, 569.
55. Kim, H. J.; Tyagi, R. K.; Fouda, A. E.; Jonasson, K. *J. Appl. Polym. Sci.* **1996**, *62*, 621.
56. Yong, S. K.; Hyo, J. K.; Un, Y. K. *J. Membr. Sci.* **1991**, *60*, 219.
57. Zheng, Q.-Z.; Wang, P.; Yang, Y.-N. *J. Membr. Sci.* **2006**, *279*, 230.
58. Mazinani, S.; Darvishmanesh, S.; Ehsanzadeh, A.; van der Bruggen, B. *J. Membr. Sci.* **2017**, *526*, 301.
59. Peng, J.; Su, Y.; Chen, W.; Shi, Q.; Jiang, Z. *Indus. Eng. Chem. Res.* **2010**, *49*, 4858.
60. Saljoughi, E.; Amirilargani, M.; Mohammadi, T. *J. Appl. Polym. Sci.* **2009**, *111*, 2537.
61. Zhang, Z.; An, Q.; Ji, Y.; Qian, J.; Gao, C. *Desalination*. **2010**, *260*, 43.
62. Kang, J. S.; Lee, Y. M. *J. Appl. Polym. Sci.* **2002**, *85*, 57.
63. Li, Z.; Ren, J.; Fane, A. G.; Li, D. F.; Wong, F.-S. *J. Membr. Sci.* **2006**, *279*, 601.
64. Ruaan, R.-C.; Chang, T.; Wang, D.-M. *J Polym Sci B*. **1999**, *37*, 1495.
65. Tsai, J. T.; Su, Y. S.; Wang, D. M.; Kuo, J. L.; Lai, J. Y.; Deratani, A. *J. Membr. Sci.* **2010**, *362*, 360.
66. Evenepoel, N.; Wen, S.; Tilahun Tsehaye, M.; van der Bruggen, B. *J. Appl. Polym. Sci.* **2018**, *135*, 46494.
67. Wang, H. H.; Jung, J. T.; Kim, J. F.; Kim, S.; Drioli, E.; Lee, Y. M. *J. Membr. Sci.* **2019**, *574*, 44.
68. Dong, X.; Al-Jumaily, A.; Escobar, I. C. *Membranes*. **2018**, *8*, 23.
69. Figoli, A.; Marino, T.; Simone, S.; Di Nicolo, E.; Li, X.-M.; He, T.; Tornaghi, S.; Drioli, E. *Green Chem.* **2014**, *16*, 4034.
70. Marino, T.; Blasi, E.; Tornaghi, S.; Di Nicolò, E.; Figoli, A. *J. Membr. Sci.* **2018**, *549*, 192.
71. Rasool, M. A.; Vankelecom, I. F. J. *Green Chem.* **2019**, *21*, 1054.
72. Amelio, A.; Genduso, G.; Vreysen, S.; Luis, P.; van der Bruggen, B. *Green Chem.* **2014**, *16*, 3045.
73. Marino, T.; Galiano, F.; Molino, A.; Figoli, A. *J. Membr. Sci.* **2019**, *580*, 224.
74. Häckl, K.; Kunz, W. *C. R. Chim.* **2018**, *21*, 572.

75. Lalia, B. S.; Kochkodan, V.; Hashaikeh, R.; Hilal, N. *Desalination*. **2013**, *326*, 77.
76. Young, T.-H.; Chen, L.-W. *Desalination*. **1995**, *103*, 233.
77. Boom, R. M.; van den Boomgaard, T.; van den Berg, J. W. A.; Smolders, C. A. *Polymer*. **1993**, *34*, 2348.
78. Xu, L.; Qiu, F. *Polymer*. **2014**, *55*, 6795.
79. Keshavarz, L.; Khansary, M. A.; Shirazian, S. *Polymer*. **2015**, *73*, 1.
80. Lau, W. W. Y.; Guiver, M. D.; Matsuura, T. *J. Membr. Sci.* **1991**, *59*, 219.
81. Zeman, L.; Tkacik, G. *J. Membr. Sci.* **1988**, *36*, 119.
82. Swinyard, B. T.; Barrie, J. A. *Br. Polym. J.* **1988**, *20*, 317.
83. Mansourizadeh, A.; Ismail, A. F. *J. Membr. Sci.* **2010**, *348*, 260.
84. Appaw, C.; Gilbert, R. D.; Khan, S. A.; Kadla, J. F. *Biomacromolecules*. **2007**, *8*, 1541.
85. Lin, K.-Y.; Wang, D.-M.; Lai, J.-Y. *Macromolecules*. **2002**, *35*, 6697.
86. Xu, Z.; Tsai, H.; Wang, H.-L.; Cotlet, M. *J. Phys. Chem. B.* **2010**, *114*, 11746.
87. Wang, L. K.; Chen, J. P.; Hung, Y.-T.; Shammas, N. K., Eds. Membrane and Desalination Technologies; New York: Springer Science & Business Media, **2011**.
88. Kahrs, C.; Metze, M.; Fricke, C.; Schwellenbach, J. *J. Mol. Liq.* **2019**, *291*, 111351.
89. Saljoughi, E.; Amirilargani, M.; Mohammadi, T. *Desalination*. **2010**, *262*, 72.
90. Moradihamedani, P.; Ibrahim, N. A.; Yunus, W. M. Z. W.; Yusof, N. A. *Polym. Eng. Sci.* **2014**, *54*, 1686.
91. Chaturvedi, B. K.; Ghosh, A. K.; Ramachandhran, V.; Trivedi, M. K.; Hanra, M. S.; Misra, B. M. *Desalination*. **2001**, *133*, 31.
92. Wijmans, H. Synthetic Membranes: On the mechanisms of formation of membranes and the concentration polarization phenomenon in ultrafiltration. Dissertation: Enschede, **1984**.
93. Lakshmi, D. S.; Figoli, A.; Buonomenna, M. G.; Golemme, G.; Drioli, E. *Adv. Polym. Technol.* **2012**, *31*, 231.